**Title: Activation of a chondrocyte volume-sensitive $Cl^-$ conductance prior to macroscopic cartilage lesion formation in the rabbit knee anterior cruciate ligament transection osteoarthritis model.**

Kosuke Kumagai[1, 2], Futoshi Toyoda[3], Caroline A Staunton[1], Tsutomu Maeda[2], Noriaki Okumura[2], Hiroshi Matsuura[3], Yoshitaka Matsusue[2], Shinji Imai[2], Richard Barrett-Jolley[1]

[1]Department of Musculoskeletal Biology, Institute of Aging and Chronic Disease, University of Liverpool

[2]Departments of Orthopedic Surgery, Shiga University of Medical Science

[3]Departments of Physiology, Shiga University of Medical Science

Total number of words in the paper, excluding references and figure legends: 3470

Name and postal and email addresses for the corresponding author:

Richard Barrett-Jolley

Department of Musculoskeletal Biology

Institute of Aging and Chronic Disease

University of Liverpool

E-mail: rbj@liverpool.ac.uk

**Running title: Early $I_{Cl,vol}$ activity in rabbit ACLT OA**

**Abstract**

**Objective:** The anterior cruciate ligament transection (ACLT) rabbit osteoarthritis (OA) model confers permanent knee instability and induces joint degeneration. The degeneration process is complex, but includes chondrocyte apoptosis and OA-like loss of cartilage integrity. Previously, we reported that activation of a volume-sensitive $Cl^-$ current ($I_{Cl,vol}$) can mediate cell shrinkage and apoptosis in rabbit articular chondrocytes. Our objective was therefore to investigate whether $I_{Cl,vol}$ was activated in the early stages of the rabbit ACLT OA model.

**Design:** Adult Rabbits underwent unilateral ACLT and contralateral arthrotomy (sham) surgery. Rabbits were euthanized at 2 or 4 weeks. Samples were analyzed histologically and with assays of cell volume, apoptosis and electrophysiological characterization of $I_{Cl,vol}$.

**Results:** At 2 and 4 weeks post ACLT cartilage appeared histologically normal, nevertheless cell swelling and caspase 3/7 activity were both significantly increased compared to sham controls. In cell-volume experiments, exposure of chondrocytes to hypotonic solution led to a greater increase in cell size in ACLT compared to controls. Caspase-3/7 activity, an indicator of apoptosis, was elevated in both ACLT 2wk and 4wk. Whole-cell currents were recorded with patch clamp of chondrocytes in iso-osmotic and hypo-osmotic external solutions under conditions where $Na^+$, $K^+$ and $Ca^{2+}$ currents were minimized. ACLT treatment resulted in a large increase in hypotonic-activated chloride conductance.

**Conclusion:** Changes in chondrocyte ion channels take place prior to the onset of apparent cartilage loss in the ACLT rabbit model of OA. Further studies are needed to investigate if pharmacological inhibition of $I_{Cl,vol}$ decreases progression of OA in animal models.

**Keywords**

Osteoarthritis; cartilage; ion channels; ACLT; chloride channel; anion channel; caspase; apoptosis

**Introduction:**

Chondrocyte apoptosis is an important contributor to the development and growth of healthy articular cartilage[1]. In the process of normal bone growth and endochondral ossification, terminally differentiated chondrocytes are removed from the calcified cartilage by apoptosis prior to the transition to bone[1]. There is also evidence that an increased incidence of chondrocyte apoptosis during aging is responsible for the hypocellularity associated with degradation and/or pathological remodeling of the cartilage matrix, and exacerbates the risk of degenerative joint diseases such as osteoarthritis (OA)[1]. Study of this in biopsies from OA patients can suffer from the limitation that OA is typically presented at an advanced stage. To address this issue, this study used a knee instability anterior cruciate ligament tear rabbit model (ACLT) which induces OA-like degradative changes in the joint[2, 3] and investigated changes in chondrocyte physiology taking place prior to apparent macroscopic changes of the cartilage.

During onset of OA, disruption of the collagen network of cartilage is also accompanied by an increase in water content and a corresponding decrease in cartilage osmolality[4, 5]. Decrease in extracellular osmolality causes chondrocytes to swell[6], and cell swelling is, in general, a trigger for apoptosis[7]. Articular chondrocytes are also exposed to perturbation of osmotic

pressure and ionic composition during normal use[6]. Chondrocytes have mechanisms in place to oppose cell swelling (referred to as regulatory volume decrease, RVD) and several ion channels and transporters have been implicated in this cell-volume regulatory process (for reviews see[6, 8] and these have been implicated in pathogenesis of OA.

In previous studies, we and others have shown that volume-sensitive $Cl^-$ channels ($I_{Cl,vol}$) are functionally expressed by articular chondrocytes and involved RVD[9-11]. Aberrant activation of $I_{Cl,vol}$ under iso-osmotic conditions contributes to the cell-shrinkage associated with induction of apoptosis in cells including chondrocytes[12, 13]. We therefore hypothesized that the chondrocyte $I_{Cl,vol}$ may also be associated with OA.

In the current report we measured *early* changes in chondrocyte volume regulation and of the volume-sensitive $Cl^-$ current ($I_{Cl,vol}$), together with an apoptotic marker (caspase activity) and cartilage histology. Our results show that $I_{Cl,vol}$, cell-volume control and caspase activity are all altered following ACLT, but prior to the manifestation of histologically detectable OA.

**Methods**

Brief methods are included below, with more detailed methods in the "**Supplementary**

84 **Methods**" document. All experimental protocols conformed to The Guide for the Care and
85 Use of Laboratory Animals (National Research Council 2011) and were approved by the
86 Animal Care and Use Committee of Shiga University of Medical Sciences. All experiments
87 used adult male white rabbits (body weight, 2.5 to 3kg). Sham and ACLT surgical induction
88 were conducted on right knees.
89
90 ***Histological examination:***
91 3μm thick sections were obtained from the femoral side of patellofemoral joints and stained
92 with toluidine blue and safranin-O as for proteoglycans and glycosaminoglycans. For overall
93 evaluation of the cartilage area, tissues were graded by 3 blinded observers using both the
94 Mankin score system[14] and OARSI histopathology score[15].
95
96 ***Isolation of rabbit articular chondrocytes:***
97 Articular chondrocytes were isolated using an enzymatic dissociation procedure similar to
98 that described previously[16] with modifications[10]. Dispersed chondrocytes were washed three
99 times, re-suspended in DMEM supplemented 40mM mannitol (~360mosmol/L) and used
100 within 8h.

***Caspase-3/7 activity measurement:***

Caspase-3/7 activity was measured as an indicator of apoptosis using the Caspase-Glo 3/7 assay system (Promega, Madison, WI, USA). The luminescent signal was measured with a luminometer (Infinite M200, Tecan, Männedorf, Switzerland).

***Cell swell assay:***

Cell size measurements and patch-clamp experiments were conducted on round-shaped chondrocytes. Live chondrocytes microscopy images were captured (at 1 min intervals) before and during a hypo-osmotic challenge at a 2560×1920 pixel resolution using a CCD digital camera (DS-Fi1, Nikon) equipped with a DS-L2 control unit (Nikon). The cell cross-sectional areas were calculated using Image-J (NIH, Bethesda, MD, USA). These were each normalized to their respective initial iso-osmotic size.

***Electrophysiology:***

Whole-cell membrane currents were recorded from isolated chondrocytes. Square-step and voltage-ramp protocols were used to record whole-cell currents. Hypotonic-isotonic

difference currents were calculated by subtracting individual currents under isotonic conditions, from the equivalents in hypotonic conditions. We calculated conductance plots using Boltzmann transformations of data to separate the underlying whole-cell ion conductance from the Ohmic driving force for ion flow. These data were then fit by Boltzmann equations[17] as follows;

$$g_{(Vm)} = \frac{g}{(1 + \exp(V_m - V_h)/k)}$$

Equation 3

where $g$ is the maximal conductance, $V_h$ is the $Vm$ at which the conductance is half-activated ( "midpoint") and $k$ is the slope of activation.

***Statistical analysis:***

Data are written as means (95% confidence intervals), with the number of animals (cell isolations) and cells from which measurements were made indicated by *N* and *n*, respectively. Statistical comparisons were made using either Student's t-test or a general linear model ANOVA (Minitab version 17, Minitab Ltd., Coventry UK) as stated.

***Solutions and Chemicals:***

The iso-osmotic external solution used for the patch-clamp experiments contained (in mM): mannitol 150, NaCl 100, $MgCl_2$ 2.0, $BaCl_2$ 2.0, $GdCl_3$ 0.03, glucose 5.5, and Hepes 10 (pH 7.4). Measured osmolality was approximately 360 mOsm. This osmolality was chosen because it resembles that of native cartilage. The pipette solution contained (in mM): caesium aspartate 135, CsCl 30, TEA-chloride 20, $MgCl_2$ 2.0, Tris-ATP 5.0, $Na_2$-GTP 0.1, EGTA 5.0, and Hepes 5.0 (pH 7.2). The iso-osmotic external solution used for measuring cell swell contained (in mM): mannitol 180, NaCl 90, KCl 5.4, $CaCl_2$ 1.8, $MgCl_2$ 0.5, $NaH_2PO_4$ 0.33, glucose 5.5, and Hepes 5.0 (pH 7.4). The hypo-osmotic external solution was made by omitting mannitol.

## Results

***Histological observation:***

2 and 4 weeks following surgical treatment, tissue slices were prepared and assessed according to both the Mankin and OARSI osteoarthritis scoring systems[14, 15]. All areas of the 2 and 4-wk specimens of the ACLT knees were found to have macroscopically normal histological appearance in both toluidine blue and safranin-O staining (Figure 1).

***Cell-volume control assay:***

To analyze whether changes in cellular phenotype had developed in chondrocytes from the macroscopically normal cartilage, we began by assessing chondrocyte cell-volume properties. We measured relative cell-volume response from isolated sham (control), ACLT 2wk and ACLT 4wk rabbit cartilage isolated chondrocytes, using our cell-swell assay. Cells were incubated in 360mOsm solution and then exposed to a (180mOsm) hypo-osmotic external solution. The degree of hypo-osmotic cell swelling was evaluated by measuring the cross-sectional area of cell images. As shown in Figure 2, exposure of a chondrocyte to hypo-osmotic solution led to a rapid increase in relative cell size (approx. 6% swell, Figure 2) compared to that in control cells. Figure 2 also shows the time-course of cell swell under these conditions. Chondrocytes from ACLT 2wk and 4wk rabbit cartilage tissue showed a more rapid increase in cell size than controls, both reaching a highly significantly greater relative volume at 5min post hypotonic challenge (approx. 8% and 11% swell respectively, Figure 2). These changes could result from a reduced capacity of chondrocytes to regulate their cellular-volume at a very early stage of OA progression.

169 ***ACLT induced caspase 3/7 activity:***

170 Changes in cellular volume regulation are frequently linked to progression of apoptosis. To
171 investigate this we used an apoptosis assay. We used a caspase-3/7 activity assay since it has
172 been previously demonstrated that this is a major step in apoptotic cell death[18].
173 As a positive control, we used TNFα treatment (24hrs 10ng/ml). We also investigated if this
174 process could be prevented by an inhibitor of the swelling/volume sensitive chloride channel
175 blocker DCPIB. TNFα induced a significant increase in caspase-3/7 activity and this was
176 abolished by DCPIB. DCPIB alone had no effect on population incidence of apoptosis. We
177 also determined incidence of apoptosis in ACLT cartilage and the controls. We found
178 caspase-3/7 activity to be significantly elevated in both 2wk and 4wk ACLT OA models
179 (Figure 3) in comparison with control.
180
181 ***Constitutive anion channel activity in ACLT chondrocytes and controls:***
182 Articular chondrocytes express a wide variety of cation and anion channels important for cell
183 volume control[8]. We recently showed a major contribution of $I_{Cl.vol}$ to drug doxorubicin-
184 induced chondrocyte apoptosis in chondrocytes[13] and so the current study focused on anion
185 currents. Isolated rabbit articular chondrocytes were investigated under conditions designed

186 to minimize $Na^+$ currents (a holding potential of −30mV), $Ca^{2+}$ currents (removal of $Ca^{2+}$
187 from the external solution), $K^+$ currents (omission of $K^+$ from the internal solution and
188 addition of $BaCl_2$ to the external solution), and electrogenic $Na^+/K^+$ pump current (omission
189 of $Na^+$ and $K^+$ from internal and external solutions, respectively). $Gd^{3+}$-sensitive stretch-
190 activated channels[19] were also blocked by adding 30 μM $GdCl_3$ to the bath. $Gd^{3+}$ also blocks
191 the majority of TRP cation channels[20]. Figure 4A and B shows representative whole-cell
192 currents under these conditions, in response to 200 ms square voltage-clamp steps applied
193 from a holding potential of −30 mV to test potentials of +80 to −100mV in 10mV steps. In
194 our previous pharmacological studies, we established this was a chloride conductance[9, 10]. To
195 allow in depth analysis of the whole-cell conductance we transformed the current-voltage
196 data to whole-cell conductance plots (Figure 4E). These were then fit with Boltzmann curves
197 (Equation 3) showing that maximum conductance ($g$) was significantly increased by ACLT
198 surgery, but that slope ($k$) and half-maximum conductance activation ($V_h$) were not
199 significantly changed (Figure 4E).
200
201 ***Hypotonicity-activated anion channel activity in ACLT chondrocytes and controls:***
202 Exposure of the chondrocyte to hypo-osmotic solution caused increase in the whole-cell

current in chondrocytes from both control and ACLT cartilage (Figure 4C, D and Figure 6C, D). The hypo-osmotic swelling-activated current was also largely time-independent at potentials negative to +50mV and outwardly rectifying with a reversal potential (Figure 4E and F) close to the calculated $E_{Cl^-}$. To investigate the molecular identity of the hypotonically activated chloride conductance, we measured difference currents of control cells with and without the presence of 3 different chloride channel blockers; $CaCC_{Inh}$-A01 (a selective blocker of the $Ca^{2+}$-activated chloride channel and TMEM16A/anoctamin-1/ANO-1)[21], DCPIB (an inhibitor of the volume sensitive anion channel[22]), VSAC/VRAC) and arachidonic acid (an inhibitor of VRAC[23]). All 3 of these caused a significant inhibition of conductance, $CaCC_{Inh}$-A01 significantly more effective than DCPIB or arachidonic acid (Figure 5).

To analyze ACLT induced changes in underlying conductance in detail, we Boltzmann transformed control and ACLT hypotonic difference currents and fitted these with Equation 3 (Figure 6E). In both controls and ACLT samples, hypotonicity results in a significant increase in maximum conductance and steeper slope (smaller absolute *k*). In control cells, the half maximum activation voltage ($V_h$) of conductance was significantly shifted to the left (channels open at more negative potentials) by hypotonic challenge. This leftward shift of *Vh*

220 was not apparent in ACLT cells. To analyze and quantify just the hypotonically activated
221 current, without contamination of the tonically active current, we constructed difference
222 currents, for currents in isotonic and hypotonic solutions. The hypo-osmotic swelling-
223 activated difference current was also outwardly rectifying with a reversal potential (Figure 4E
224 and F) close to $E_{Cl^-}$. We Boltzmann transformed and fitted the hypotonic-isotonic difference
225 currents in control and ACLT chondrocytes (Figure 7). The difference current maximum
226 conductance ($g$) was significantly greater in ACLT chondrocytes and shifted to the right
227 compared to controls. The slope of activation was not significantly different.
228
229 **Discussion**
230 In this study we used a rabbit joint destabilization model of early arthritis. We investigated
231 samples prior to the development of macroscopic cartilage changes, but found that caspase-
232 3/7 activity (apoptosis), cell-volume regulation and the chloride conductance $I_{Cl,vol}$ were all
233 significantly altered in ACLT treatment joints compared to sham controls.
234
235 The diagnosis of OA is mainly based on physical examination and radiograph (Kellgren-
236 Lawrence grading (K-L Grading)) supported by laboratory tests such as C-reactive protein

237 (CRP), erythrocyte sedimentation rate (ESR) or arthroscopy. Each of these diagnostic
238 techniques has limitations: Radiographs provide positive results only after significant
239 progression of disease[24]. C-reactive protein and ESR are indicators of inflammation, but are
240 not site specific. Arthroscopy reveals damage to cartilage that is not visible on radiographs,
241 but is an invasive technique. Magnetic resonance imaging is a useful alternative and non-
242 invasive technique, but cost and availability can prevent routine use. Joint tissue degeneration
243 is therefore usually advanced by the time the diagnosis and our research focus has shifted to
244 understand the earliest physiological changes in cartilage or chondrocytes.

245 ***Histological Analysis of control and post ACLT samples***

246 Our histological data convincingly show no significant difference in indicators of
247 degeneration between any of the three groups using the Mankin score system[14] or OARSI
248 histopathology score[15]. These histological results are consistent with previous reports. For
249 whilst a previous study did observe degenerative changes 4 weeks post ACLT, they were
250 much less marked than longer term studies and there was no evidence of full-thickness
251 ulceration. In addition, those changes that were observed were quite variable between
252 samples[3]. Therefore, it appears that 4-week post-ACLT is, in rabbits, somewhat of a threshold
253 stage of OA where macroscopic changes just begin to materialize.

***Changes in cell volume properties***

Despite the lack of clear macroscopic histological changes in the 2 or 4-week ACLT cartilage samples, we did find a number of changes in chondrocyte cellular physiology. What triggers these changes prior to evident changes in matrix structure is unknown; possibilities include changes in mechanical loading of cartilage and thus resident chondrocytes[25], or very early biochemical changes and induced stress, several of which have been shown to change early in models of OA[26, 27]. Potentially, even the established changes in cartilage osmolality[4] could lead to secondary changes in chondrocyte phenotype. Since chondrocytes produce the enzymes that maintain cartilage, it seems logical that changes in chondrocyte phenotype could precede evident extracellular matrix changes. The first observation we made was that chondrocytes swelled more following ACLT treatment than sham controls. Since passive cell swell and RVD take place in parallel, this phenomenon could be due to a decreased capacity for RVD (which would otherwise oppose cell swell), a change in cytoskeletal properties, or an increase in cell membrane permeability to water which could arise from the increased aquaporin expression we previously reported to occur in some models of OA[28]. These hypotheses are not mutually exclusive, since it is likely that changes in any of the components of cell-volume regulation, such as aquaporins, $I_{Cl.vol}$, BK etc[8] could lead to an

impaired ability to undergo RVD.

***Changes in apoptosis***

One key consequence of altered cell-volume regulation is programmed cell death, apoptosis[29, 30]. Other important elements of the apoptotic pathway are the activity of a number of intracellular enzymes including the caspases[31]. We chose to investigate caspase activity, with a luminescence system optimized for detection of isoforms 3/7, since it is thought that all apoptosis pathways pass through these[31]. Our data showed that caspase-3/7 activity was increased at both 2-weeks and 4-weeks following ACLT confirming again, that cellular physiological changes had taken place prior to observable macroscopic degeneration.

***Electrophysiological changes***

Several ion channels are involved with chondrogenesis[32], chondrocyte migration[33], volume control/ apoptosis[34, 35] and mechanotransduction[36]. Considerable interest has also surrounded the chondrocyte stretch activated BK channel[8, 37, 38] and TRPV4 cation channels[39-41], with TRPV4 being raised as a potential therapeutic target in a range of musculoskeletal diseases[42]. Anion channels are, however, equally important to cation channels and some of our own previous work has shown that a swell activated chloride channel $I_{Cl,vol}$ is of particular importance to development of apoptosis in chondrocytes[13]. Our previous

288 electrophysiological studies showed that $I_{Cl,vol}$ (also referred to as the volume-sensitive
289 organic osmolyte/anion) is functionally expressed in rabbit articular chondrocytes and is
290 involved in cell volume maintenance mechanisms such as RVD[9, 10]. In addition to this
291 physiological importance in the homeostatic regulation of cell volume, activation of $I_{Cl,vol}$ has
292 also been suggested to contribute to the cell shrinkage associated with apoptosis in several
293 cell types[12].
294 In the present study we measured whole-cell currents in conditions optimized for detection of
295 chloride conductances (e.g., potassium free etc). We analyzed currents under both isotonic
296 conditions and following hypotonic shock. Both "resting" (iso-osmotic) and hypotonic-
297 activated currents were increase significantly in cells from joints 4 weeks post ACL. Detailed
298 analysis reveals that hypotonic challenge of chondrocytes changed the maximum chloride
299 conductance, the slope and midpoint for voltage activation of this conductance. Changes to
300 all three of these parameters is fully consistent with the idea that hypotonicity activates a
301 chloride conductance that is not present under isotonic conditions in control chondrocytes
302 (i.e., $I_{Cl,vol}$ *see Figure 4*). Conversely, ACLT treatment significantly increased only the
303 maximal conductance of chondrocytes without significantly changing either slope or
304 midpoint of its activation; consistent with the hypothesis that there has been an increase in the

number of active $I_{Cl,vol}$ channels, rather than a change in their electrophysiological properties or expression of an entirely new/different channel. It is also consistent with a hypothesis that there has been an activation of $I_{Cl,vol}$, even under isotonic conditions. Calculation of Boltzmann parameters from hypotonic-isotonic difference currents removes any contribution from constitutively active background conductances active under isotonic conditions.

Previously, two clearly distinguishable phenotypes of anion channels have been linked to cell apoptosis and cell volume regulation; the volume-regulated anion channel (VRAC) and the calcium-activated chloride conductance (CaCC)[23, 43]. Molecular identities have proven elusive with several gene products having been proposed; CLCN3 (CLC3), bestrophin, ANO-1 (an anoctamin) and the LRRC8 family[43, 44]. Latest evidence suggests that ANO-1 is synonymous with CaCC[43, 45] and LRRC8 gene family products contribute to VRAC[46, 47]. The correlation between gene and functional channel identity is still somewhat unclear however, since there is also evidence to state that LRRC8 gene products are *non*-critical to VRAC function[48]. Our own recent qPCR studies of human cartilage show the presence of chloride channels CLCN-3, CLCN-7 and bestrophin, but we were not able to analyze either the anoctamin or LRRC8 families[49]. Here, we attempted to identify the underlying phenotype of $I_{Cl,vol}$ using a pharmacological approach, since rabbit chloride channel gene sequences are not

322 yet well characterized. There are no truly selective drugs for chloride channels, but DCPIB is
323 considered somewhat selective for VRAC relative to other volume-activated chloride channel
324 candidates such as CLC-3 and ANO-1[22]. Arachidonic acid is also thought to inhibit VRAC,
325 but not ANO-1[23]. Conversely, $CaCC_{Inh}$-A01 is thought selective for CaCC[21] compared to
326 VRAC. We chose optimal concentrations of agents, based on the literature quoted above and
327 found both arachidonic acid and DCPIB to powerfully inhibit control $I_{Cl,vol}$. Interestingly, the
328 apparently selective ANO-1 inhibitor CaCCInh-A01 also inhibited $I_{Cl,vol}$ albeit significantly
329 less potently than inhibitors of VRAC. Tentatively, our data suggests that both ANO-1- like
330 and VRAC-like conductances may contribute to $I_{Cl,vol}$. Comparison of Boltzmann parameters
331 between control and ACLT chondrocytes shows a large increase in maximum conductance,
332 but no change in slope (*see Figure 7*). There is also, in this case, a shift of midpoint for
333 voltage activation to the right (more positive potentials). This is surprising given the lack of
334 shift in midpoint of the raw Boltzmann and supports the hypothesis that, following ACLT
335 treatment, there is a substantial proportion of $I_{Cl,vol}$ channel active under isotonic conditions,
336 i.e., even before the application of hypotonic stretch. In all these scenarios, using an
337 electrophysiological approach, it is not possible to determine if the profound increases in
338 chloride conductance associated with ACLT result from the increased cell swell (shown in

339 Figure 2) or are independent of this. That there appears to be an increase of $I_{Cl,vol}$ activity
340 even under isotonic conditions following ACLT, may suggest the latter; increased functional
341 expression. There are no direct proteomic or transcriptomic data for the rabbit ACLT OA
342 model, but there is considerable evidence of changes in anion channel expression and DNA
343 methylation in human studies, albeit of OA at advanced stages of progression. Specifically,
344 recent microarray studies revealed significant changes in ANO-1/TEMEM16A[28].
345 Furthermore, LRRC8 genes also appear profoundly different in human OA. Next
346 generation sequencing shows a 2.4 fold increase in LRRC8D (*adjusted p-val* 1.05e-6[50]) and
347 fascinatingly, this is matched by a differentially methylation loci within LRRC8 genes[51].
348 Conversely, the hypo-osmotic state of more advanced degenerating cartilage itself may be
349 expected to have an opposing effect on overall chloride conductance (i.e., decreasing chloride
350 conductance), since *in vitro* studies, subjecting a human chondrocyte cell line to hypo-
351 osmotic stress decreased expression of CLC-7/CLCN7[52], a chloride channel especially
352 involved with acid-base regulation.
353 In the light of these data, we hypothesize that increased activation of $I_{Cl,vol}$ may occur at an
354 early stage of OA and persist through its progression. Since volume-activated channels
355 contribute to cell shrinkage, and cell shrinkage is a key component of apoptosis, this may be

356 associated with the increase in caspase 3/7 activity. It should be noted, however, that we
357 applied a hypo-osmotic solution for only a few minutes, whilst naturally, patients would have
358 a decrease in joint fluid osmolality for many years. Future studies will be needed to
359 determine if chloride channel inhibitor drugs or biologics are able to reduce progression of
360 OA in pre-clinical models.
361
362 **Acknowledgments**
363 We would like to thank Mrs. Yoko Uratani for her support during this study. This work was
364 supported by Grant-in-Aid for Young Scientists (B) from Japan Society for the Promotion of
365 Science (JSPS) (26861185), UK Royal Society (IE140240) and the Gen Foundation.
366
367 **Author Contributions**
368 (1) The conception and design of the study, or acquisition of data, or analysis and
369 interpretation of data: KK FT CAS TM NO HM YM SI RBJ.
370 (2) Drafting the article or revising it critically for important intellectual content:
371 KK FT CAS TM NO HM YM SI RBJ.
372 (3) Gave final approval of the version to be submitted: KK FT CAS TM NO HM YM

373 SI RBJ.

374

375 **Role of Funding Source**

376 The funders had no role in the design, data collection and analysis, decision to publish, or the

377 preparation of the manuscript.

378

379 **Conflict Of Interest**

380 None of the authors has any conflict of interest in the outcomes of this study.

381

382

**References:**


1 Mobasheri A. Role of chondrocyte death and hypocellularity in ageing human articular cartilage and the pathogenesis of osteoarthritis. Med Hypotheses 2002; 58: 193-197.

2 Brandt KD, Myers SL, Burr D, Albrecht M. Osteoarthritic changes in canine articular cartilage, subchondral bone, and synovium fifty-four months after transection of the anterior cruciate ligament. Arthritis Rheum 1991; 34: 1560-1570.

3 Yoshioka M, Coutts RD, Amiel D, Hacker SA. Characterization of a model of osteoarthritis in the rabbit knee. Osteoarthritis Cartilage 1996; 4: 87-98.

4 Maroudas A, Venn M. Chemical composition and swelling of normal and osteoarthrotic femoral head cartilage. II. Swelling. Ann Rheum Dis 1977; 36: 399-406.

5 Guilak F, Erickson GR, Ting-Beall HP. The effects of osmotic stress on the viscoelastic and physical properties of articular chondrocytes. Biophys J 2002; 82: 720-727.

6 Bush PG, Hall AC. Regulatory volume decrease (RVD) by isolated and in situ bovine articular chondrocytes. J Cell Physiol 2001; 187: 304-314.

7 Lang F, Hoffmann EK. CrossTalk proposal: Cell volume changes are an essential step in the cell death machinery. J Physiol 2013; 591: 6119-6121.

8 Lewis R, Asplin KE, Bruce G, Dart C, Mobasheri A, Barrett-Jolley R. The role of the membrane potential in chondrocyte volume regulation. J Cell Physiol 2011; 226: 2979-2986.

9 Isoya E, Toyoda F, Imai S, Okumura N, Kumagai K, Omatsu-Kanbe M, et al. Swelling-activated $Cl^-$ current in isolated rabbit articular chondrocytes: inhibition by arachidonic Acid. J Pharmacol Sci 2009; 109: 293-304.

10 Okumura N, Imai S, Toyoda F, Isoya E, Kumagai K, Matsuura H, et al. Regulatory role of tyrosine phosphorylation in the swelling-activated chloride current in isolated rabbit articular chondrocytes. J Physiol 2009; 587: 3761-3776.

11 Ponce A, Jimenez-Pena L, Tejeda-Guzman C. The role of swelling-activated chloride currents (I(CL,swell)) in the regulatory volume decrease response of freshly dissociated rat articular chondrocytes. Cell Physiol Biochem 2012; 30: 1254-1270.

12 Okada Y, Shimizu T, Maeno E, Tanabe S, Wang X, Takahashi N. Volume-sensitive chloride channels involved in apoptotic volume decrease and cell death. J Membr Biol 2006; 209: 21-29.

13 Kumagai K, Imai S, Toyoda F, Okumura N, Isoya E, Matsuura H, et al. 17ß-Estradiol inhibits the doxorubicin-induced apoptosis via block of volume-sensitive Cl− current in rabbit articular chondrocytes. British Journal of Pharmacology 2012; 166: 702-720.

14 Mankin HJ, Dorfman H, Lippiello L, Zarins A. Biochemical and metabolic abnormalities in articular cartilage from osteo-arthritic human hips. II. Correlation of morphology with biochemical and metabolic data. J Bone Joint Surg Am 1971; 53: 523-537.

15 Pritzker KP, Gay S, Jimenez SA, Ostergaard K, Pelletier JP, Revell PA, et al. Osteoarthritis cartilage histopathology: grading and staging. Osteoarthritis Cartilage 2006; 14: 13-29.

16 Wilson JR, Duncan NA, Giles WR, Clark RB. A voltage-dependent K+ current contributes to membrane potential of acutely isolated canine articular chondrocytes. J Physiol 2004; 557: 93-104.

17 Barrett-Jolley R, Pyner S, Coote JH. Measurement of voltage-gated potassium currents in identified spinally-projecting sympathetic neurones of the paraventricular nucleus. Journal of Neuroscience Methods 2000; 102: 25-33.

18 Nicholson DW, Thornberry NA. Caspases: killer proteases. Trends in Biochem Sciences 1997; 22: 299-306.

19 Yellowley CE, Hancox JC, Donahue HJ. Effects of cell swelling on intracellular calcium and membrane currents in bovine articular chondrocytes. J Cell Biochem 2002; 86: 290-301.

20 Pedersen SF, Owsianik G, Nilius B. TRP channels: an overview. Cell Calcium 2005; 38: 233-252.

21 De La Fuente R, Namkung W, Mills A, Verkman AS. Small-molecule screen identifies inhibitors of a human intestinal calcium-activated chloride channel. Mol Pharmacol 2008; 73: 758-768.

22 Decher N, Lang HJ, Nilius B, Bruggemann A, Busch AE, Steinmeyer K. DCPIB is a novel selective blocker of I(Cl,swell) and prevents swelling-induced shortening of guinea-pig atrial action potential duration. Br J Pharmacol 2001; 134: 1467-1479.

452 23 Hoffmann EK, Holm NB, Lambert IH. Functions of volume-sensitive and
453 calcium-activated chloride channels. IUBMB Life 2014; 66: 257-267.
454 24 Garnero P, Piperno M, Gineyts E, Christgau S, Delmas PD, Vignon E.
455 Cross sectional evaluation of biochemical markers of bone, cartilage, and
456 synovial tissue metabolism in patients with knee osteoarthritis: relations
457 with disease activity and joint damage. Ann Rheum Dis 2001; 60: 619-626.
458 25 Guilak F. Biomechanical factors in osteoarthritis. Best Practice &
459 Research in Clinical Rheumatology 2011; 25: 815-823.
460 26 Goldring MB, Goldring SR. Osteoarthritis. Journal of Cellular Physiology
461 2007; 213: 626-634.
462 27 Goldring MB. The role of the chondrocyte in osteoarthritis. Arthritis and
463 Rheumatism 2000; 43: 1916-1926.
464 28 Lewis R, May H, Mobasheri A, Barrett-Jolley R. Chondrocyte channel
465 transcriptomics: do microarray data fit with expression and functional
466 data? Channels (Austin) 2013; 7: 459-467.
467 29 Maeno E, Ishizaki Y, Kanaseki T, Hazama A, Okada Y. Normotonic cell
468 shrinkage because of disordered volume regulation is an early prerequisite
469 to apoptosis. Proc Natl Acad Sci U S A 2000; 97: 9487-9492.
470 30 Bortner CD, Cidlowski JA. A necessary role for cell shrinkage in apoptosis.
471 Biochem Pharmacol 1998; 56: 1549-1559.
472 31 Thornberry NA, Lazebnik Y. Caspases: enemies within. Science 1998; 281:
473 1312-1316.
474 32 Fodor J, Matta C, Olah T, Juhasz T, Takacs R, Toth A, et al. Store-
475 operated calcium entry and calcium influx via voltage-operated calcium
476 channels regulate intracellular calcium oscillations in chondrogenic cells.
477 Cell Calcium 2013; 54: 1-16.
478 33 Matta C, Fodor J, Miosge N, Takacs R, Juhasz T, Rybaltovszki H, et al.
479 Purinergic signalling is required for calcium oscillations in migratory
480 chondrogenic progenitor cells. Pflugers Arch 2015; 467: 429-442.
481 34 Lewis R, Feetham C, Barrett-Jolley R. Cell volume control in chondrocytes.
482 Cellular Physiology and Biochemistry 2011; 28: 1111-1122.
483 35 Lewis R, Feetham CH, Gentles L, Penny J, Tregilgas L, Tohami W, et al.
484 Benzamil sensitive ion channels contribute to volume regulation in canine
485 chondrocytes. British Journal of Pharmacology 2013; 168: 1584-1596.
486 36 Lee W, Leddy HA, Chen Y, Lee SH, Zelenski NA, McNulty AL, et al.

487 Synergy between Piezo1 and Piezo2 channels confers high-strain
488 mechanosensitivity to articular cartilage. Proceedings of the National
489 Academy of Sciences 2014; 111: E5114-E5122.
490 37 Mobasheri A, Lewis R, Maxwell JEJ, Hill C, Womack M, Barrett-Jolley R.
491 Characterization of a stretch-activated potassium channel in chondrocytes.
492 Journal of Cellular Physiology 2010; 223: 511-518.
493 38 Funabashi K, Ohya S, Yamamura H, Hatano N, Muraki K, Giles W, et al.
494 Accelerated Ca2+ entry by membrane hyperpolarization due to Ca2+-
495 activated K+ channel activation in response to histamine in chondrocytes.
496 American Journal of Physiology-Cell Physiology 2010; 298: C786-C797.
497 39 Phan MN, Leddy HA, Votta BJ, Kumar S, Levy DS, Lipshutz DB, et al.
498 Functional characterization of TRPV4 as an osmotically sensitive ion
499 channel in porcine articular chondrocytes. Arthritis and Rheumatism
500 2009; 60: 3028-3037.
501 40 O'Conor CJ, Leddy HA, Benefield HC, Liedtke WB, Guilak F. TRPV4-
502 mediated mechanotransduction regulates the metabolic response of
503 chondrocytes to dynamic loading. Proc Natl Acad Sci U S A 2014; 111:
504 1316-1321.
505 41 Clark AL, Votta BJ, Kumar S, Liedtke W, Guilak F. Chondroprotective role
506 of the osmotically-sensitive ion channel TRPV4: Age- and sex-dependent
507 progression of osteoarthritis in Trpv4 deficient mice. Arthritis Rheum
508 2010; 10: 2973-2983.
509 42 McNulty AL, Leddy HA, Liedtke W, Guilak F. TRPV4 as a therapeutic
510 target for joint diseases. Naunyn Schmiedebergs Arch Pharmacol 2015;
511 388: 437-450.
512 43 Kunzelmann K. TMEM16, LRRC8A, bestrophin: chloride channels
513 controlled by Ca(2+) and cell volume. Trends Biochem Sci 2015; 40: 535-
514 543.
515 44 Fischmeister R, Hartzell HC. Volume sensitivity of the bestrophin family
516 of chloride channels. J Physiol 2005; 562: 477-491.
517 45 Terashima H, Picollo A, Accardi A. Purified TMEM16A is sufficient to form
518 Ca2+-activated Cl- channels. Proc Natl Acad Sci U S A 2013; 110: 19354-
519 19359.
520 46 Qiu Z, Dubin AE, Mathur J, Tu B, Reddy K, Miraglia LJ, et al. SWELL1, a
521 plasma membrane protein, is an essential component of volume-regulated

anion channel. Cell 2014; 157: 447-458.
47 Voss FK, Ullrich F, Münch J, Lazarow K, Lutter D, Mah N, et al. Identification of LRRC8 Heteromers as an Essential Component of the Volume-Regulated Anion Channel VRAC. Science 2014; 344: 634-638.
48 Sirianant L, Wanitchakool P, Ousingsawat J, Benedetto R, Zormpa A, Cabrita I, et al. Non-essential contribution of LRRC8A to volume regulation. Pflugers Arch 2016; 468: 805-816.
49 Asmar A, Barrett-Jolley R, Werner A, Kelly Jr R, Stacey M. Membrane channel gene expression in human costal and articular chondrocytes. Organogenesis 2016.
50 Xu Y, Barter MJ, Swan DC, Rankin KS, Rowan AD, Santibanez-Koref M, et al. Identification of the pathogenic pathways in osteoarthritic hip cartilage: commonality and discord between hip and knee OA. Osteoarthritis Cartilage 2012; 20: 1029-1038.
51 Rushton MD, Reynard LN, Barter MJ, Refaie R, Rankin KS, Young DA, et al. Characterization of the Cartilage DNA Methylome in Knee and Hip Osteoarthritis. Arthritis and Rheumatology 2014; 66: 2450-2460.
52 Kurita T, Yamamura H, Suzuki Y, Giles WR, Imaizumi Y. The ClC-7 Chloride Channel Is Downregulated by Hypoosmotic Stress in Human Chondrocytes. Molecular Pharmacology 2015; 88: 113-120.

544 **Figure Legends**

545 **Figure 1: Cartilage histology following ACLT.** Histological findings after Safranin O (A,

546 C, E) and toluidine blue (B, D, F) staining in the 3 groups (sham (control) (A, B), ACLT 2w

547 (C, D) and ACLT 4w (E, F)). Scale bar: 2 mm. All areas of ACLT 2-week and 4-week were

548 preserved with normal appearance. Mankin score and OARSI score were also normal.

549

550

**Figure 2: Control and ACLT Chondrocyte Swell Data.** Changes in cell (chondrocyte) cross-sectional area in cells from sham (blue circles), and ACLT after 2 weeks (ACLT 2W, yellow circles) and 4 weeks (ACLT 4W, red triangles). Isotonic (360 mOsm) solution was changed to hypotonic solution (180 mOsm) at time 0s. Exposure of chondrocytes to hyposmotic solution led to a rapid increase in relative cell size (6% swell; i.e., 1.06, 95% CI 1.021 – 1.099 at 5 min, n =15, N =5) in control cells, and this swell was significantly greater with cells from ACLT 2W and 4W tissue (ACLT 2wk; 1.08, 95% CI 1.060 - 1.020 at 5 min, n =21, N =5, $p \leq 0.0005$: ACLT 4wk; 1.11, 95% CI 1.071 - 1.149 at 5 min, n =11, N =5, $p \leq 0.0005$. There was no significant change in absolute initial volumes (control 875, 95% CI 848 – 902µm; ACLT 2wk 726, 95% CI 707 - 745µm and ACLT 4wk 935, 95% CI 915 – 955µm). All *p-values* were obtained from Dunnett's *post-hoc* multiple comparison against control).

565 **Figure 3: Caspase-3/7 activity, measured from chondrocytes.** Caspase activity is given in
566 terms of luminescent intensity (arbitrary units) measured with the Caspase-glo 3/7 assay
567 system described in the methods. Columns represent cells from control tissue, ACLT 2 and
568 4w represent that from tissue 2 and four weeks after ACLT. Control +TNFα is a positive
569 control where control rabbit chondrocytes were exposed to 10ng/ml TNFα for 24hr, Control +
570 DCPIB is a negative control (cells exposed to 20μM DCPIB). Control + TNFα + DCPIB
571 combines the TNFα and DCPIB treatments, as described for the previous columns. Asterisks
572 represent data significantly increased from control (Minitab GLM ANOVA, Dunnett's
573 multiple comparison *post hoc* test ** $p \leq 0.0005$). Caspase-3/7 activity was markedly elevated
574 in chondrocytes from ACLT 2w (1.24, 95% CI 1.20 - 1.28, n =20, N =5, $p \leq 0.0005$), 4w (1.52,
575 95% CI 1.40 - 1.64, n =20, N =5, $p \leq 0.0005$) animals and Control + TNFα (2.15, 95% CI 2.09
576 - 2.21, n =20, N =5, $p \leq 0.0005$). There was no significant increase from control with either
577 DCPIB alone, or TNFα +DCPIB). Note, the increase between 2wk and 4wk was also
578 statistically significant $p=0.0026$. Each cell numbers $1 \times 10^5$ cells/ml.
579

**Figure 4: Control chondrocyte whole-cell data.** Switch from isotonic solution to hypotonic solution (as described in the methods) resulted in increased whole-cell conductance in chondrocytes from sham control rabbit tissue. Solutions optimized for detection of chloride conductances (*see methods*). (A) Representative continuous raw current data trace during switch from isotonic to hypo and then hypertonic solution. Constant ramps (dV/dt 0.25V/s) were applied at 6s intervals, with full current voltage protocols run at points indicated by "a" and "c" (see B to E). (B) Expanded view of the raw current voltage data shown in (Aa,b). The upper panel illustrates the voltage protocol; the lower traces "a" and "b" are the resultant current traces. Superimposed current traces are in response to 200 ms square-steps applied from a holding potential of −30 mV to test potentials of +80 through −100 mV in 10 mV steps. (C) Mean current voltage data from a number of protocols such as that shown in A and B. The filled black circles indicate recordings in isotonic solution. There is a large activation of current in the presence of hypotonic solution (filled blue circles). (D) Subtraction of the current in isotonic from the current in hypotonic solution gives the hypotonic activated (difference) current. Current reverses near to the calculated reversal potential for chloride ions ($E_{Cl^-}$19mV). (E) Boltzmann transformation of the current-voltage curves in C (junction potential corrected data). Control isotonic data (black filled circles) is fit with midpoint ($V_h$)

40 (95% CI 16.5 - 63.5) mV, slope (*k*) 62 (95% CI 42.4 - 81.6) mV and maximum conductance (*g*) of 364 (95% CI 268 - 460) pS/pF. In hypotonic solution (blue filled circles), the mean control chondrocyte Boltzmann curve is significantly; shifted to the left ($V_h$ = -2, 95% CI -11.8 - 7.8 mV, $p \leq 0.0005$), steeper slope (*k* =31, 95% CI 23.2 - 38.8 mV $p$=0.018 and larger (maximum conductance *g* = 1350, 95% CI 1250 - 1450 pS/pF $p$=0.009). Note that these are Benjamini-Hochberg adjusted *p-values*.

**Figure 5: Pharmacological analysis of the hypotonically activated conductance.**

Hypotonic difference currents, recorded and calculated as in Figure 4D. Empty circles are under control conditions, solid circles in the presence of 20 μM CaCCinh-A01, solid triangles in the presence of 20μM DCPIB and empty circles in the presence of 30μM arachidonic acid (AA). * $p$=0.007, ** $p$<0.0005 general linear model ANOVA (Vm * drug) with Tukey's Pairwise multiple comparisons (post-hoc) test. This pairwise comparison test also revealed that the difference curves for DCPIB and AA were significantly more inhibited than that in the presence of CaCCinh-A01 (*p*-values =0.012 and 0.020 respectively). DCPIB and AA curves were not themselves significantly different.

613 **Figure 6: Whole-cell data from ACLT 4wk chondrocytes.** (A) Raw data from the same
614 protocol as that described in Figure 4, but using chondrocytes from 4W ACLT animals.
615 Switching from isotonic solutions to hypotonic solutions activates a large voltage-gated
616 current, with full current voltage protocols (see B to E) run at points indicated by "a" and "b".
617 (B) Expanded view of the raw current voltage data shown in (Aa,b). The upper panel
618 illustrates the voltage protocol; the lower traces "a" and "b" are the resultant current traces.
619 (C) Mean current voltage data from a number of protocols such as that shown in A and B.
620 Currents recorded in isotonic solution are shown as black filled circles. There is a large
621 activation of current in the presence of hypotonic solution (red filled circles). (D) Subtraction
622 of the current in isotonic from the current in hypotonic solution gives the hypotonic activated
623 (difference) current. As Figure 4, this current reverses near to the calculated $E_{Cl-}$. (E)
624 Boltzmann transformation of the current-voltage curves in C. 4wk ACLT isotonic data (black
625 filled circles) is fit with midpoint ($V_h$) 23 95% CI (-0.5 – 46.5) mV, slope 42 (95% CI 34 –
626 50) mV. These are not significantly different to the control isotonic equivalent values
627 ($p$=0.35 and $p$=0.11 respectively). Isotonic maximum conductance (762, 95% CI 58 - 966
628 pS/pF) was significantly greater than that of control chondrocytes ($p$=0.004). In hypotonic
629 solution (red filled circles), the mean 4W ACLT chondrocyte Boltzmann curve was not

630 significantly shifted ($V_h$ 10, 95% CI 2.2 – 17.8 mV) from that in isotonic ($p$=0.35) or that or

631 from the control hypotonic values ($p$=0.22), but was significantly steeper slope ($k$ 25, 95% CI

632 21.1 – 28.9 mV $p$=0.014) and larger (maximum conductance 2290, 95% CI 2200 - 2380

633 pS/pF $p \leq 0.0005$) than the ACLT isotonic conductance curves. The ACLT hypotonic

634 conductance value was also greater than the control equivalent ($p \leq 0.0005$), but not

635 significantly steeper (p=0.263). Note that these are Benjamini-Hochberg adjusted *p-values*.

636 Direct comparison of difference current derived Boltzmann curves between Control and 4 W

637 ACLT are shown in Figure 6.

638

**Figure 7: Boltzmann analysis of control and 4W ACLT difference currents:** Boltzmann curves created from the Control (blue circles) and 4W ACLT (red circles) chondrocyte difference current data shown in Figures 4 and 5. The smooth lines are fits with the Boltzmann curves with parameters as follows: For control; $V_h$ 68 (95% CI 58.2 - 77.8) mV, slope 31 (95% CI 23.16 - 58.84) mV, maximum conductance 1035 (95% CI 935 - 1135) pS/pF. For 4W ACLT curves the mean fitted parameters were: $V_h$ 7 (95% CI -2.8 - 16.8) mV, slope 24 (20.8 - 27.92) mV, maximum conductance 2290 (2200 - 2380) pS/pF. Slope was not significantly different from control ($p$=0.19), but both midpoint and maximum conductance were $p \leq 0.0005$ for each). Note that these *p-values* are Benjamini-Hochberg adjusted.

Figure 1

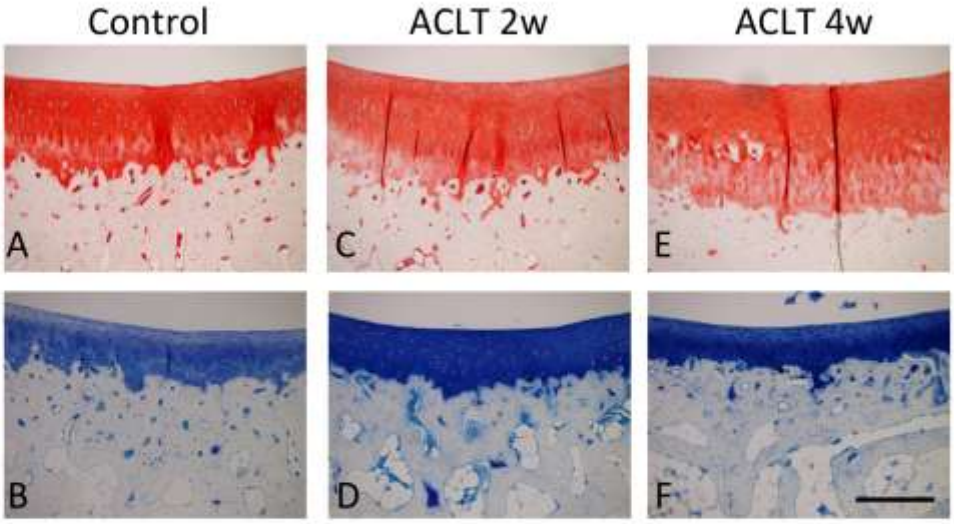


| | Control | ACLT 2w | ACLT 4w |
|---|---|---|---|
| Mankin score | 0 | 0 | 0 |
| OARSI score | 0 | 0 | 0 |

650

Figure 2

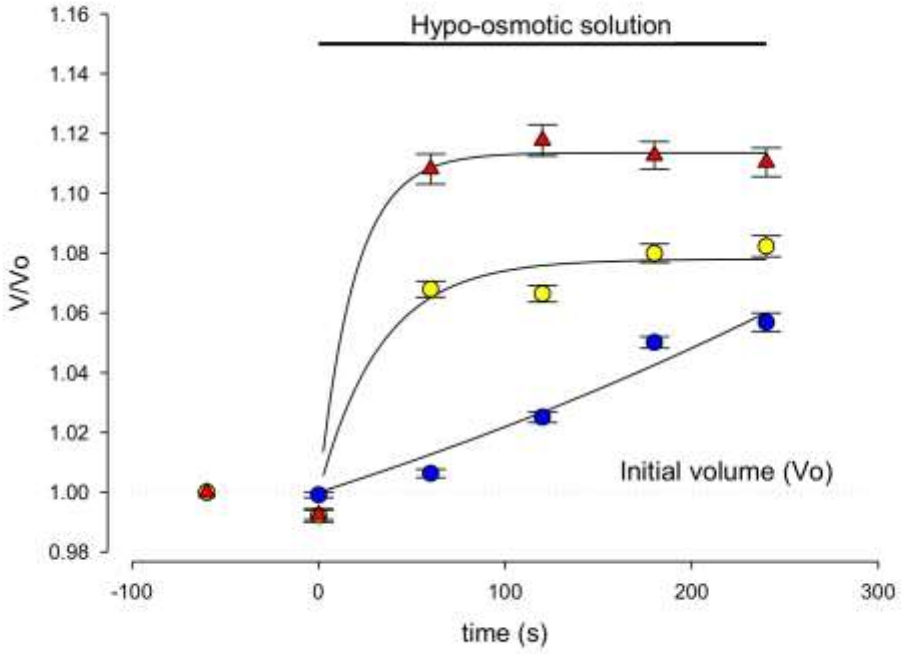


651

Figure 3

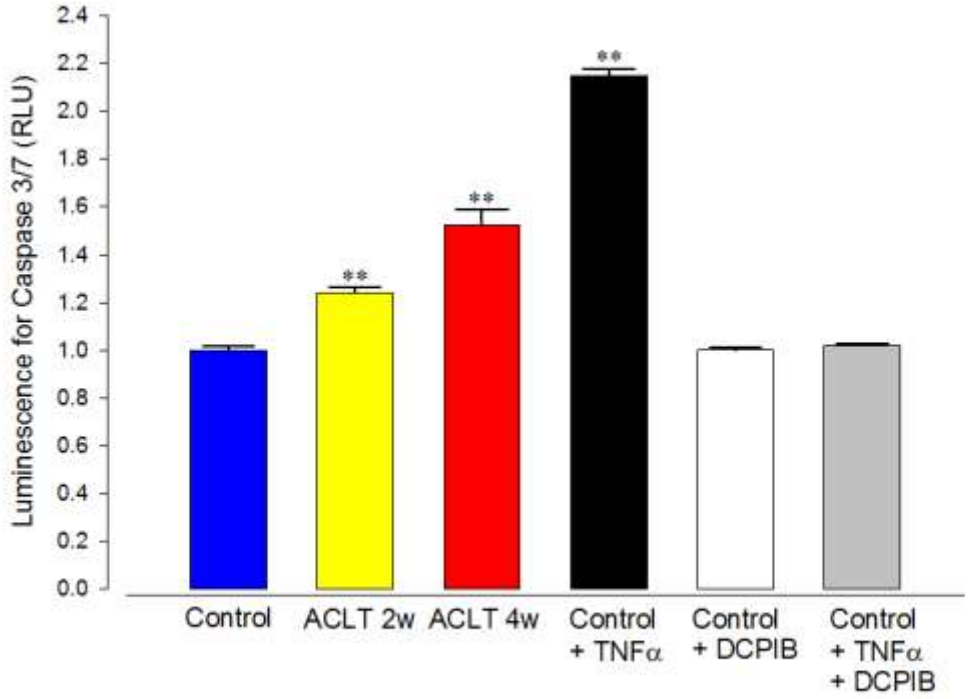


652

Figure 4

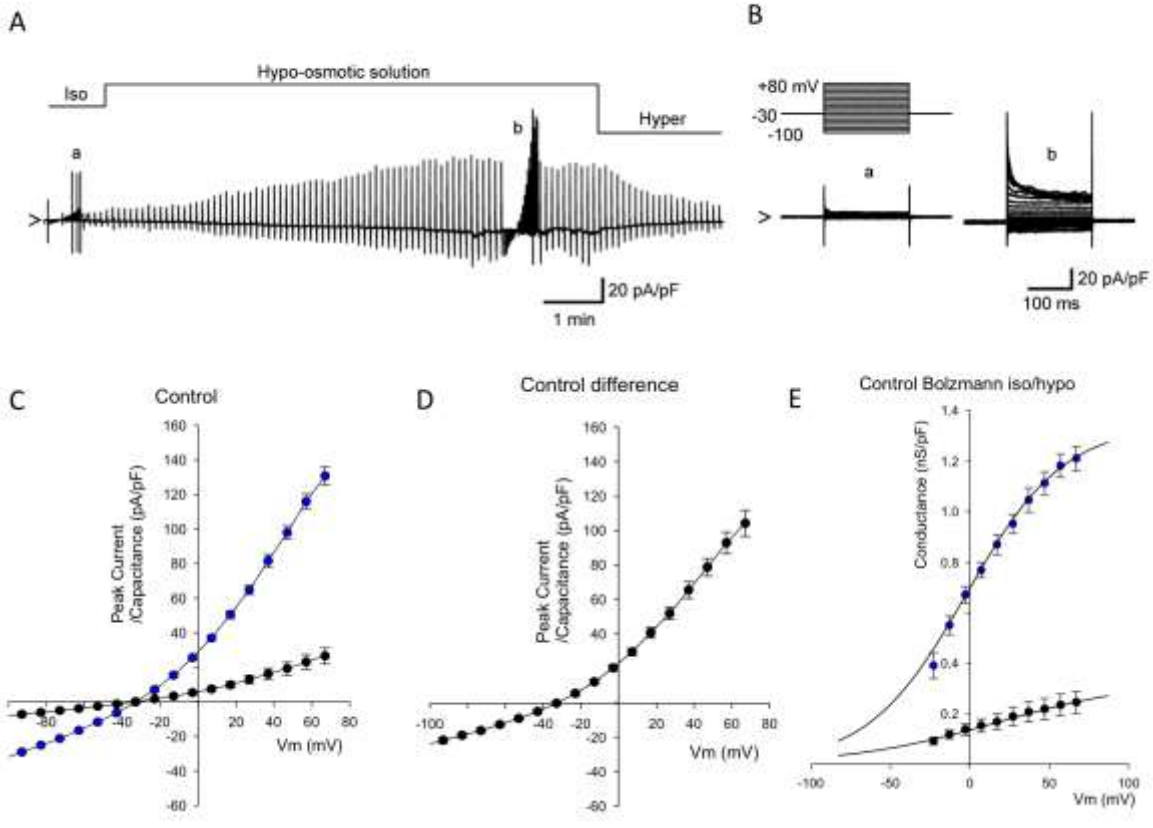


653

Figure 5

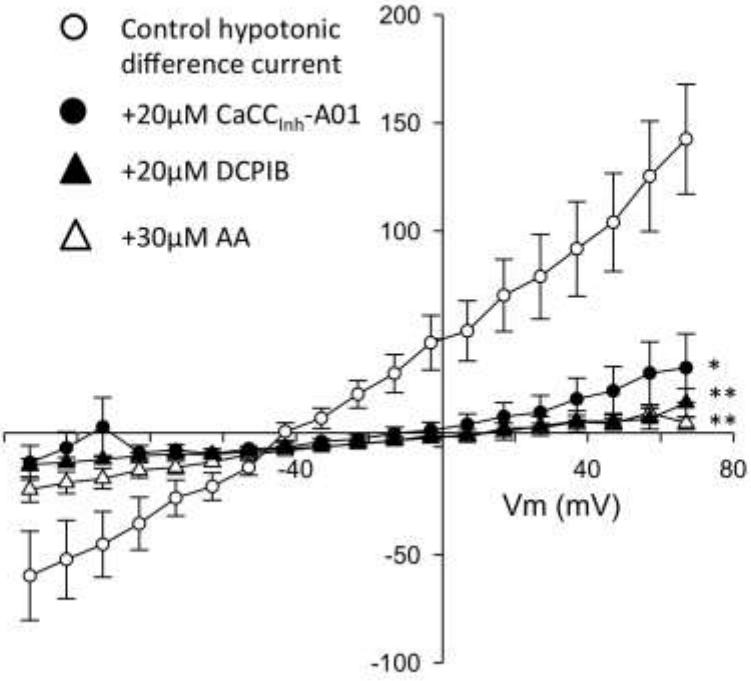


654

Figure 6

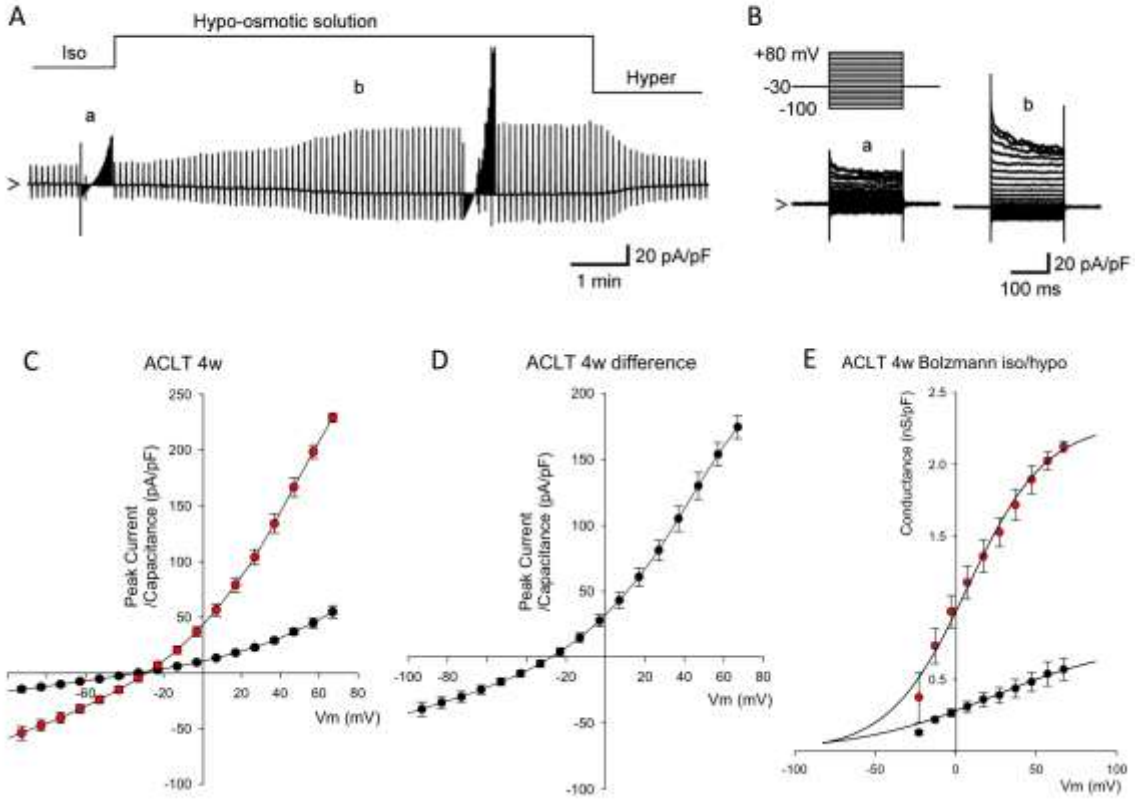


655

Figure 7

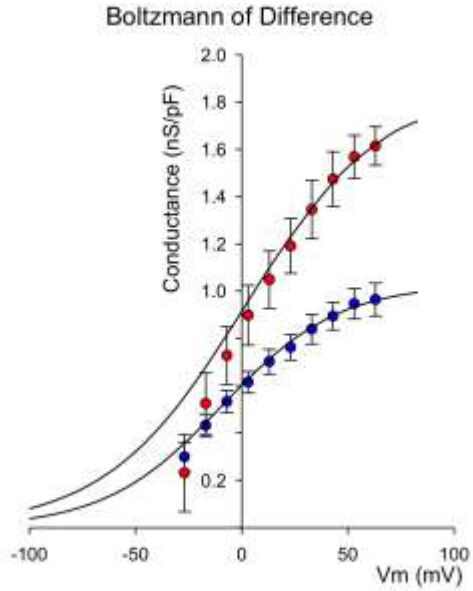
Boltzmann of Difference
Conductance (nS/pF)
2.0
1.8
1.6
1.4
1.2
1.0
0.2
-100
-50
0
50
100
Vm (mV)

656